SLEEPJ, 2021, S11–S19

doi: 10.1093/sleep/zsaa269
Advance Access Publication Date: 27 February 2021
Supplement

SUPPLEMENT

Model-based analysis of implanted hypoglossal nerve stimulation for the treatment of obstructive sleep apnea

Matthew D. Johnson[1,*,†], Yazan M. Dweiri[2,†], Jason Cornelius[3], Kingman P. Strohl[4], Armin Steffen[5], Maria Suurna[6], Ryan J. Soose[7], Michael Coleman[8], John Rondoni[8], Dominique M. Durand[9], Quan Ni[8]

[1]Department of Biomedical Engineering, University of Minnesota, Minneapolis, MN [2]Department of Biomedical Engineering, Jordan University of Science and Technology, Irbid, Jordan [3]Minneapolis Clinic of Neurology and North Memorial Help Sleep Medicine, Maple Grove, MN [4]Division of Pulmonary, Critical Care, and Sleep Medicine, Louis Stokes Veterans Affairs Medical Center and Case Medical Center, Case Western Reserve University, Cleveland, OH [5]Department of Otorhinolaryngology, University of Lübeck, Lübeck, Germany [6]Department of Otolaryngology-Head and Neck Surgery, Weill Cornell Medicine, New York, NY [7]Department of Otolaryngology, University of Pittsburgh, Pittsburgh, PA [8]Inspire Medical Systems, Inc., Minneapolis, MN [9]Department of Biomedical Engineering, Case Western Reserve University, Cleveland, OH

*Corresponding author. Matthew D. Johnson, 7-105 Nils Hasselmo Hall, 312 Church Street SE, Minneapolis, MN 55455. Email: john5101@umn.edu.

†These authors contributed equally to this work.

Abstract

Study Objectives: Individuals with obstructive sleep apnea (OSA), characterized by frequent sleep disruptions from tongue muscle relaxation and airway blockage, are known to benefit from on-demand electrical stimulation of the hypoglossal nerve. Hypoglossal nerve stimulation (HNS) therapy, which activates the protrusor muscles of the tongue during inspiration, has been established in multiple clinical studies as safe and effective, but the mechanistic understanding for why some stimulation parameters work better than others has not been thoroughly investigated.

Methods: In this study, we developed a detailed biophysical model that can predict the spatial recruitment of hypoglossal nerve fascicles and axons within these fascicles during stimulation through nerve cuff electrodes. Using this model, three HNS programming scenarios were investigated including grouped cathode (---), single cathode (o-o), and guarded cathode bipolar (+-+) electrode configurations.

Results: Regardless of electrode configuration, nearly all hypoglossal nerve axons circumscribed by the nerve cuff were recruited for stimulation amplitudes <3 V. Within this range, monopolar configurations required lower stimulation amplitudes than the guarded bipolar configuration to elicit action potentials within hypoglossal nerve axons. Further, the spatial distribution of the activated axons was more uniform for monopolar versus guarded bipolar configurations.

Conclusions: The computational models predicted that monopolar HNS provided the lowest threshold and the least sensitivity to rotational angle of the nerve cuff around the hypoglossal nerve; however, this setting also increased the likelihood for current leakage outside the nerve cuff, which could potentially activate axons in unintended branches of the hypoglossal nerve.

Clinical Trial Registration: NCT01161420.

Statement of Significance

While hypoglossal nerve stimulation is an established therapy for treating obstructive sleep apnea, the anatomical rationale for choosing one stimulation setting over another has not been thoroughly investigated. In this study, we constructed a detailed biophysical model to simulate the effects of various stimulation configurations on recruitment of axonal activity within fascicles of the hypoglossal nerve. The results provide a basis to understand the strengths and weaknesses of using monopolar versus bipolar stimulation; moreover, the data-driven modeling approach provides a framework for future studies to investigate the role other stimulation settings have on the success of selective recruitment of axonal pathways within the HGN.

Key words: obstructive sleep apnea; hypoglossal nerve stimulation; computational model; stimulation settings; electrode configuration; nerve cuff

Submitted: 24 July, 2020; **Revised:** 12 November, 2020

Introduction

Obstructive sleep apnea (OSA), which affects over 18 million adults in the United States [1], is characterized by frequent sleep disruptions that stem from tongue muscle relaxation and airway blockage. The standard of care for treating OSA is the use of positive airway pressure (PAP) systems, which while effective, are limited by high non-adherence rates that range from 46% to 83% [2]. Hypoglossal nerve stimulation (HNS) is established as another safe and effective treatment option for patients with moderate to severe OSA, especially for those who cannot adhere to PAP in both controlled study [3] and clinical practice [4, 5]. These studies have shown HNS reduced OSA severity as well as improved daytime sleepiness and other quality of life measures that are associated with OSA [3–6].

The main functional outcomes of HNS for OSA involve activating the protrusor muscles of the tongue, including the genioglossus muscle, while avoiding activation of retractor muscles, including the styloglossus and hyoglossus muscles [7]. Clinical data support the importance of selective recruitment of protrusor muscles, which was shown to yield a more favorable therapy response than mixed activation of both protrusor and retractor muscles of the tongue [8]. In addition to selective recruitment, the degree of anterior movement of the tongue has also been found to be a key predictor of responders to HGN therapy [7]. The clinical challenge then is to identify the stimulation parameters that will achieve both selective and robust activation of the protrusor muscles of the tongue.

Computational models can be helpful to improve our conceptual understanding of why some stimulation parameters work better than others [9]. In this study, we developed a detailed biophysical computational model that can simulate recruitment of fascicles and axons within fascicles during HNS with model parameters that were tuned to fit previously collected clinical data from the *Stimulation Therapy for Apnea Reduction* (STAR) trial (ClinicalTrials.gov identifier: NCT01161420) [3].

Computational models that simulate the biophysics of peripheral nerve stimulation [10–14] have shown utility for other clinical applications, including coordinating lower limb movement through femoral nerve stimulation [15], restoring bladder function through pudendal nerve stimulation [16], and treating epilepsy through vagus nerve stimulation [17, 18], among others. Such computational models have provided a number of insights into optimizing the arrangement of active electrodes as well as the shape and pattern of the stimulation pulses to recruit or block activity within a nerve [9]. Previous studies have leveraged such approaches to improve targeting of individual fascicles [19], more selective recruitment of axons based on their diameter [20, 21], and better control over the directionality of stimulus-induced action potentials propagating along axons within a nerve fiber [22]. Such approaches that leverage computational models provide a framework for future advances in HNS therapy and have direct clinical applicability to optimizing patient outcomes.

The model framework consisted of (1) a finite element model predicting the spatial distribution of tissue voltages resulting from electrical stimulation through one or more electrodes along a nerve cuff, and (2) biophysical cable models of axons that can predict the effects of electrical stimulation on axonal transmembrane currents including the generation of action potentials [10, 23]. These models were then used to investigate the role of stimulation amplitude and electrode configuration (i.e. combination of cathode(s) and anode(s)) in activating axons within the hypoglossal nerve. While there are numerous stimulation parameters that one can test when programming a patient with a hypoglossal nerve stimulator, this study provides important context for why stimulation parameters may be more or less beneficial for HNS therapy.

Methods

Modeling the fascicular structure of the hypoglossal nerve

The human hypoglossal nerve is monofascicular at its proximal and middle portions and polyfascicular at its distal end near the innervation points in the geniohyoid and genioglossus muscles of the tongue [24] (Figure 1A). Previous studies have noted that near the distal end, there is one primary fascicle surrounded by one or more smaller accessory fascicles [25]. For this study, a histological cross-section of the hypoglossal nerve was

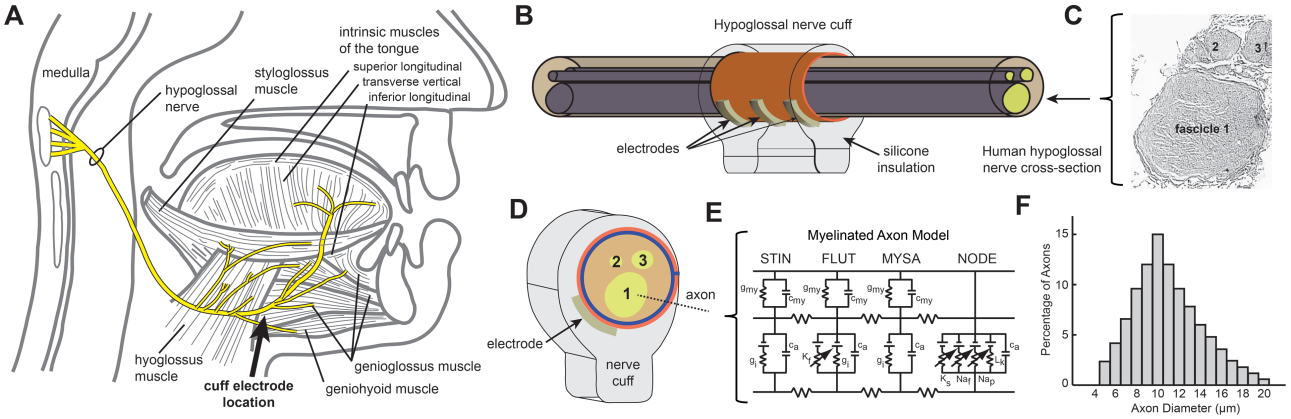

Figure 1. Computational model of hypoglossal nerve stimulation. (A) Nerve cuff placement between the nerve branches to the hyoglossus and genioglossus muscles. (B) The nerve cuff consisted of three electrodes arranged along the hypoglossal nerve, which (C) consisted of several fascicles at its distal portion [25]. (D) Nerve reconstruction within the cuff showing a primary fascicle and two accessory fascicles. (E) Axonal membrane dynamics within the fascicles were modeled using a multicompartment equivalent circuit cable model approach. (F) The biophysical models incorporated a range of axonal diameters. Histological image in part (C) reprinted with permission from Springer.

segmented to include three fascicles of 1,422, 711, and 457 μm diameters (Figure 1B and C). Surrounding each of these fascicles was a perineurium layer with a thickness defined as 3% of the fascicle diameter (42.7, 21.3, and 13.7 μm, respectively) [26]. The nerve was modeled with an overall diameter of 2.4 mm and epineurium filling in the space amongst the fascicles. These cross-sectional features were extruded 9.1 cm in length such that the nerve extended approximately 2 cm on either side of the nerve cuff.

Modeling the hypoglossal nerve cuff interface

The distal portion of the hypoglossal nerve, particularly distal to the styloglossus and hyoglossus branching points [27], has been the primary surgical target for placement of a nerve cuff along the hypoglossal nerve. The clinical nerve cuff had an inner diameter of 3.1 mm as well as a 130 μm slit along its length to minimize compression of the nerve. Within the nerve, cuff were three curved strip electrodes (1.22 mm length, 1.46 mm^2 exposed surface area) with 3.68 mm center-to-center spacing along the length of the cuff. Surrounding these electrodes were insulated layers of silicone. The orientation of the cuff electrodes with respect to the hypoglossal nerve was such that 0° corresponded to a cuff placement in which the largest fascicle was located immediately adjacent to the cuff electrodes (Figure 1D).

Implantation of a nerve cuff is known to induce an inflammatory response that generates a fibrous tissue encapsulation around the nerve and around the implanted cuff. The thickness and cellular morphology of this encapsulation tissue depend on the shape of the cuff as well as the surface texture and material composition of the implant [28]. The tissue consists of a combination of macrophages, foreign body giant cells, loose collagen, and fibroblasts with impedances sufficient to alter the shape and magnitude of the electric field generated by chronically implanted electrodes [29]. Based on previous reports showing postmortem encapsulation layers in canines [30], we incorporated a 300 μm thick layer of encapsulation tissue attached to the inner cuff wall and a thicker 1.2 mm layer of encapsulation tissue attached to the external surface of the nerve cuff. Between the nerve and the encapsulation layer, a 50 μm layer of interstitial fluid was also included.

Finite element model of HGN stimulation

An important component to understanding the effects of HGN stimulation is knowing how electrical current propagates through the complex tissue medium within and surrounding the HGN. The three-dimensional reconstructions of the hypoglossal nerve and cuff interface were thus incorporated into finite element model (FEM, COMSOL Multiphysics v5.3a) with inhomogeneous (i.e. location-dependent) and anisotropic (i.e. orientation-dependent) electrical conductivities that encompassed components of the nerve, cuff-electrode, and surrounding tissue. The FEM geometries were assigned electrical conductivity properties of the endoneurium, perineurium, epineurium, encapsulation tissue within and around the cuff interface, and interstitial fluid with values consistent with previous computational models of peripheral nerve stimulation [26] (Table 1). Incorporation of encapsulation tissue on the external portions of the nerve cuff was found to be important for aligning the model results to the clinical outcomes. The tissue distal from the nerve-cuff interface was assigned an average conductivity of 0.2 S/m.

Table 1. Electrical conductivity properties of the HGN stimulation model

Structure	Conductivity (S/m)
Perineurium	0.0021
Endoneurium	
Longitudinal	0.5714
Transverse	0.0826
Epineurium	0.0826
Encapsulation	0.008
Interstitial fluid	2.0

An outer tissue bounding box of 25 mm on each side was incorporated around the nerve and cuff interface. The union of geometries meshed with Delaunay tesselation and a variable resolution of tetrahedral elements ranging from 50 μm to 9 mm, which resulted in approximately 1.5 million elements. These mesh sizes were such that increasing the mesh resolution resulted in less than 1% change in the predicted tissue voltages within the nerve cuff.

Voltage-controlled stimulation was modeled for monopolar electrode configurations by setting one or more electrodes as the cathode and the bottom "neck" panel of the tissue bounding box as the anode. The other panels as well as the insulation of the nerve cuff were assigned Neumann boundary conditions of zero flux. The monopolar configurations evaluated in the model included a single centered cathode (o-o) and a grouped cathode (---), in which the cathode(s) were located within the nerve cuff and the anode was the neurostimulator metallic shell implanted below the clavicle. The bipolar configuration simulated in this study was a guarded cathode (+-+) in which both cathode and anodes are within the nerve cuff. These three settings represent nearly all of the electrode configurations used in clinical practice. For each of these electrode configurations, a stationary simulation was run to estimate the peak tissue voltages resulting during electrical stimulation. These simulations solved the Poisson equation using the direct solver in COMSOL Multiphysics v5.3a.

Axonal models of hypoglossal nerve stimulation

Another important component to understanding the effects of HGN stimulation is knowing how the time-varying, spatially nonuniform tissue voltages influence axons within the HGN. The human hypoglossal nerve holds approximately 9,000 axons at its proximal location [24], and likely half as many at its distal location where the nerve cuff is located. While it is possible to model and simulate all membrane activity within all axons of the hypoglossal nerve, one can greatly reduce the density of axons without losing much resolution in the overall percentage of axons activated by a particular stimulation setting. In this study, a total of 214 axons were modeled (n = 166 for fascicle 1, n = 35 for fascicle 2, and n = 13 for fascicle 3).

Multicompartment cable models of the myelinated axons were constructed in the programming environment NEURON (v7.3) with explicit geometrical and biophysical representations of the nodes of Ranvier, myelin attachment sections of the paranode,

main section of the paranode, and internodal sections under the Schwann cells [11] (Figure 1E). To assess the relationship between axon diameter and recruitment thresholds, a distribution of axon diameters were modeled (range from 5 to 20 μm diameter, peak at 10 μm) (Figure 1F). The internodal spacing of these axons was set as 100× the axon diameter, which is consistent with calculations from peripheral nerves [31]. This distribution of axon diameters was randomly populated within the three fascicles.

The extracellular stimulus waveform was formulated by passing the biphasic waveform (used in the Inspire Medical Systems voltage-controlled neurostimulator) through an equivalent circuit model of the electrode-tissue interface and then scaling the waveform according to the extracellular tissue voltages calculated from the FEM at each axonal membrane compartment. The biphasic waveform had a 92.4 μs stimulus phase, followed by a 244.5 μs interphase delay, and then a recharge phase that was either 754 μs in duration (bipolar configurations) or 620 μs (monopolar configurations).

These waveforms were incorporated into the e_extracellular mechanism in NEURON, which calculates and applies the transmembrane currents induced by the extracellular stimulus perturbations along the axon. A membrane voltage probe was inserted into the distal end of the axon, which was in the direction of the geniohyoid and genioglossus muscles. A stimulus train of five pulses was simulated for a given stimulus waveform, amplitude, and electrode configuration. If the membrane voltage exceeded –20 mV, which was the threshold used in this study for detecting an action potential, and did so for at least four of the five stimulus pulses, the axon was defined as "activated." A binary search algorithm was used to identify the stimulation voltage threshold for each modeled axon within the nerve. For each stimulation configuration and amplitude, a population response was calculated from these threshold values.

Clinical evaluation of hypoglossal nerve stimulation thresholds

Retrospective analysis of stimulation thresholds was performed based on clinical evaluations from human patients implanted with HGN stimulation systems. HNS was defined with respect to tongue motion at two threshold levels. The first was a sensation threshold, given by the lowest stimulation amplitude that a patient-perceived tongue motion. The second was a functional threshold for bulk tongue movement observed through the oral cavity and over the frontal teeth [32]. These threshold data across multiple different stimulation cathode and anode configurations served as outcome measures to optimize the modeling parameters.

Results

Clinical evaluation of hypoglossal nerve stimulation thresholds

Clinical HNS thresholds were compiled from a previously published trial [3] to compare three different electrode configurations: guarded cathode (+–+), single cathode (o–o), and grouped cathode (–––). Using the guarded cathode configuration, the average sensation threshold was 1.3 ± 0.8 V and increased to 2.2 ± 1.0 V for functional thresholds (Figure 2A). In comparison, the monopolar configurations of (o-o) and (---) resulted in reduced sensation thresholds and functional thresholds. In both cases, the relative ratio of stimulation thresholds between the monopolar configurations and the guarded bipolar configuration was consistent for both sensation and functional thresholds.

Calibration of computational models using clinical thresholds

Tissue encapsulation conductance was modified in the models to simulate the guarded cathode setting yielding the highest thresholds and the grouped cathode setting yielding the lowest thresholds. The conductance was also modified (tuned to 0.008 S/m) in order for the model-based sensation thresholds, which were defined as activation of 15% of HGN axons, and model-based functional thresholds, which were defined as activation of 85% of HGN axons, were consistent between electrode configurations (Figure 3). The sensation thresholds were found to predominantly activate the largest diameter axons in the nerve for both grouped cathode and guarded cathode configurations, whereas the functional thresholds activated a broad range of axon diameters.

Hypoglossal nerve activation depends on electrode configuration

The distribution of activated axons within the hypoglossal nerve was more uniform for monopolar (--- and o-o configurations)

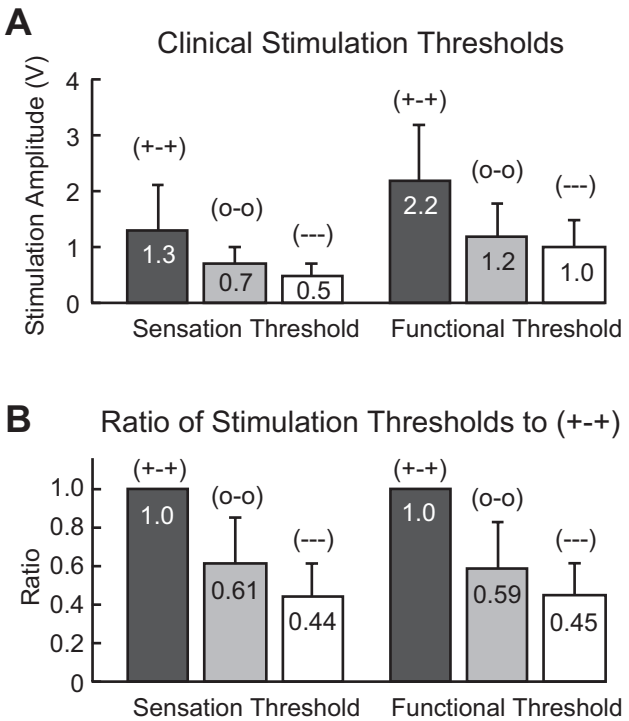

Figure 2. Clinical hypoglossal nerve stimulation thresholds. (A) Stimulation amplitude thresholds for both perception of tongue muscle contraction by the patient (sensation) and observation of tongue muscle contraction by the clinician (functional). (B) Relative thresholds for single cathode (o-o) and grouped cathode (---) configurations in comparison to the guarded cathode configuration (+-+). Thresholds were collected from 52 patients for (+-+), 28 for (o-o) and 38 for (---).

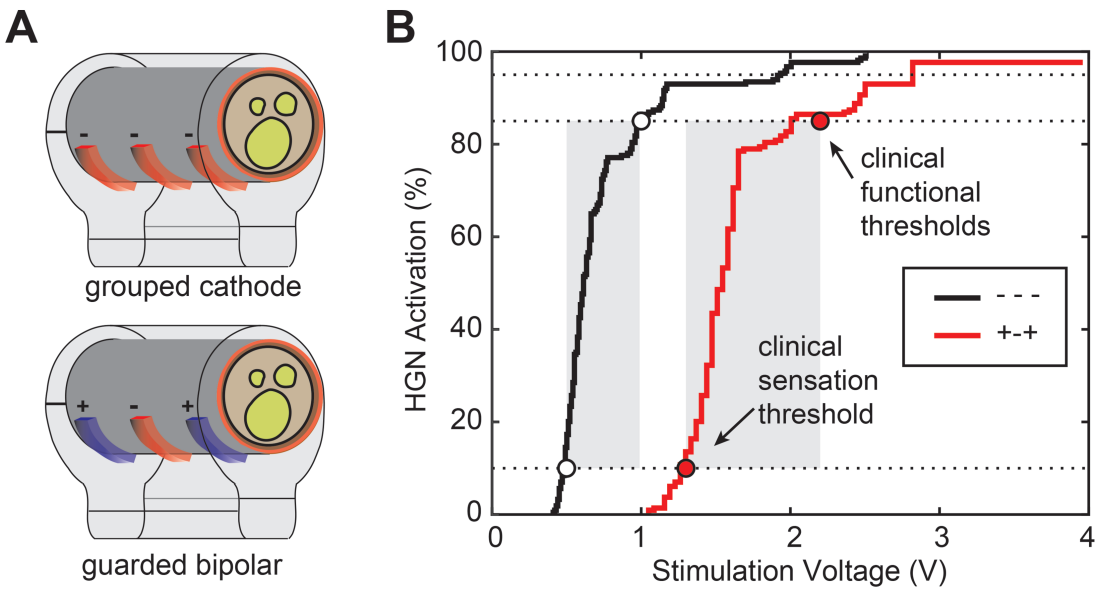

Figure 3. Effects of electrode configuration on hypoglossal nerve activation. Shown are thresholds for grouped cathode (---) and guarded cathode bipolar (+-+) configurations. Clinical sensation and functional thresholds are from Figure 2 and consistent in the model with 15% and 85% activation of the axons within the hypoglossal nerve.

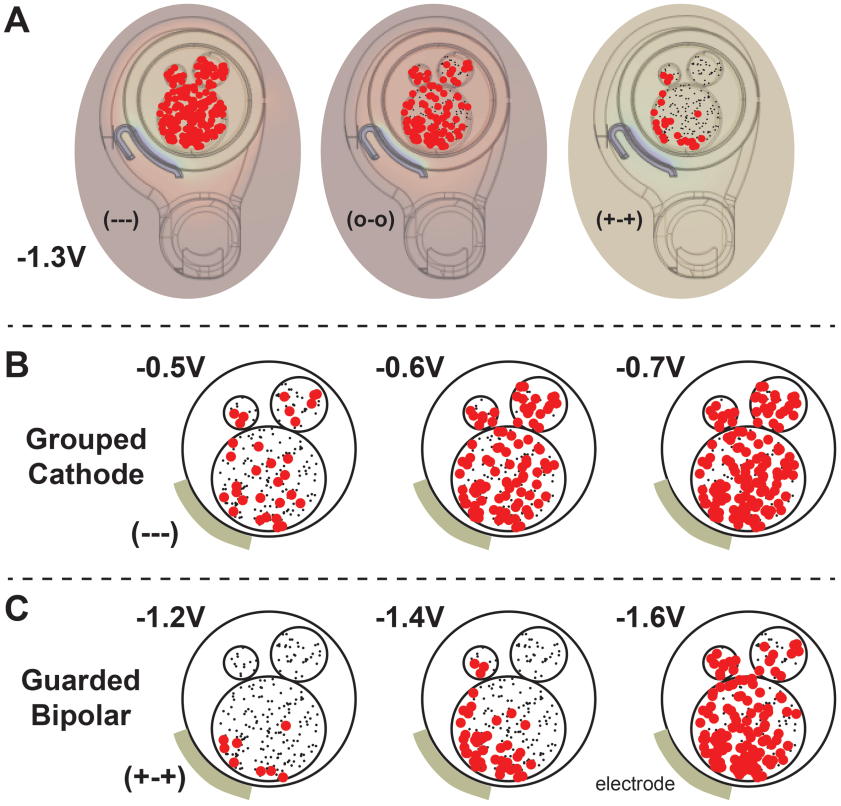

Figure 4. Comparison of the spatial distribution of axon activation within the hypoglossal nerve amongst grouped cathode (---), single cathode (o-o), and guarded cathode (+-+) configurations. Shown are A, spatial activation at −1.3 V for each configuration, as well as amplitude sweeps for B, grouped cathode and C, guarded cathode configurations.

than for bipolar (+-+) stimulation settings (Figure 4A). As stimulation amplitude increased for the monopolar configurations, the distribution of activation was first characterized by capture of large-diameter axons throughout all three fascicles (Figure 4B). As stimulation amplitude was further increased, the density of activation within each fascicle also increased such that smaller diameter axons were in turn recruited at higher stimulation amplitudes. In contrast, the guarded bipolar configuration was characterized by a spatial activation profile in which activated axons were located proximal to the electrodes

within the nerve cuff (Figure 4C). Again, as stimulation amplitudes increased, the density of activation also increased within the hypoglossal nerve, but in comparison to the monopolar configurations, this followed a pattern of axonal activation that was more aligned with axonal proximity to the active electrodes than axonal diameter.

Monopolar electrode configurations are less sensitive to hypoglossal nerve orientation

Given the propensity of guarded bipolar configurations to have nonuniform spatial activation profiles within the hypoglossal nerve, we investigated how axonal activation depends on the nerve orientation with respect to the cuff electrodes (Figure 5). For all three fascicles, axonal activation using the grouped cathode configuration had minimal dependency on nerve orientation within the cuff. This grouped cathode configuration also showed a relatively steep uptick in axonal activation once reaching a critical threshold of around 0.4 V for all three fascicles. The guarded bipolar configuration, however, had a much greater dependency on the rotation of the nerve cuff, especially for the two smaller fascicles. Additionally, the likelihood of axonal activation with bipolar stimulation had a more gradual increase in increasing stimulation amplitude.

Discussion

While HNS is an established therapy for treating OSA, the physiological rationale for choosing one stimulation setting over another has not been thoroughly investigated. In this study, we constructed a detailed biophysical model to simulate the effects of various stimulation configurations on recruitment of axonal activity within the hypoglossal nerve. The results provide a basis to understand the strengths and weaknesses of using monopolar versus bipolar stimulation; moreover, the computational modeling approach provides a framework for future studies to investigate the role other stimulation settings have on the success of selective recruitment of axonal pathways within the HGN.

One of the primary findings in this study was that monopolar stimulation generated a uniform spatial pattern of axonal recruitment within all three modeled fascicles with the lowest thresholds for activation reserved for the largest diameter axons. This suggests that the initial "sensation" thresholds reported by the patient correspond to activation of these large diameter axons and that the distribution of the sensed muscle activation is likely to be broad in distribution. Additionally, given that the "functional" threshold amplitudes of stimulation were found to be approximately twice as large (~1.0 V versus ~0.5 V, Figure 2) as the "sensation" thresholds, it is also likely that to achieve a positive functional outcome, one needs to recruit axons across a wide range of axonal diameters within the HGN.

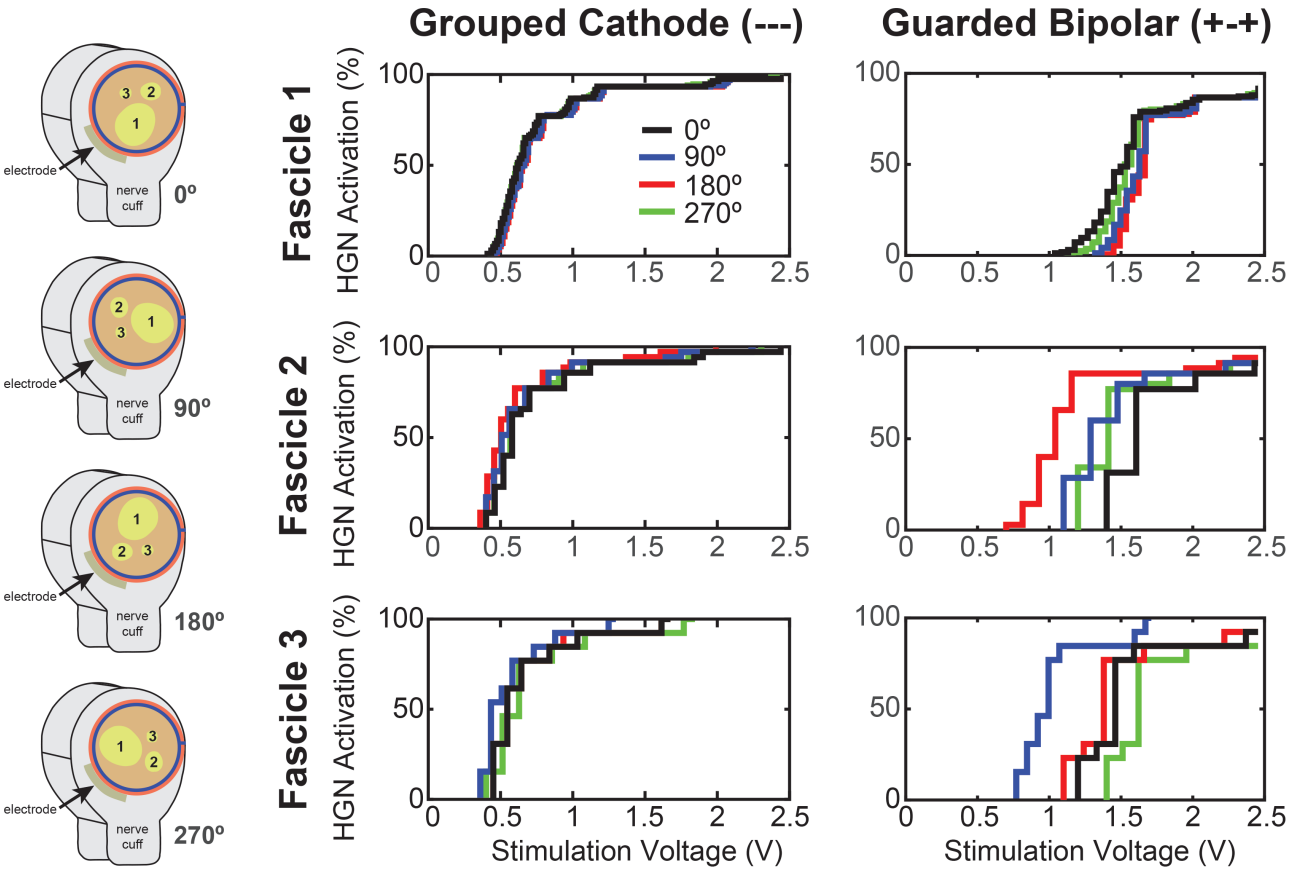

Figure 5. Effects of hypoglossal nerve orientation on axonal activation for grouped cathode (---) and guarded cathode (+-+) configurations. Shown are activation profiles for nerve orientations for 0° (primary fascicle is proximal to the cuff electrodes), 90°, 180°, and 270°.

The models also indicated monopolar stimulation results in relatively high current densities at the nerve cuff end such that the resulting electric field lines project parallel to the nerve. Both high current densities and electric field orientation along a nerve have been shown to be important contributors to axonal activation [12, 23]. Thus, when a nerve cuff is positioned near nerve branches to the styloglossus and hyoglossus muscles, there would be a higher likelihood that stimulation may inadvertently activate these branches resulting in a muted or antagonizing effect on tongue motion patterns and the ability to open a patient's airway [33]. In such a case, one would want to have more selective stimulation of only the fascicles projecting to the genioglossus muscle and/or use a guarded bipolar configuration to constrain the current within the nerve cuff.

In comparison to the monopolar stimulation configurations, the guarded bipolar configuration proved to be more capable of selective activation of individual nerve fascicles that were proximal to the electrodes within the nerve cuff. Guarded bipolar configurations are often used during the initial activation protocol after nerve cuff implantation, and the models suggested that the approach may be useful to explore the relationships between tongue motion patterns and more selective fascicular activation especially in the context of cuff rotation. The effects of nerve cuff rotation on HGN activation were most prominent for the two smaller fascicles, which suggests that tongue motion patterns underlying stimulation of the small fascicular branches may be especially susceptible to the rotation of the cuff [34]. Additionally, in retrospective analysis, a more lateral rotated electrode position was associated with a higher presence of right protrusion and bilateral protrusion of the tongue, which is associated with better apnea–hypopnea index reduction [8, 33]. Cases in which there are changes in tongue motion patterns over time have been implicated in having a higher likelihood of being subprime responders [33].

If a nerve cuff were placed in a location distal to the nerve branches of the styloglossus and hyoglossus muscles, one may want to activate all fascicles contained within the nerve cuff to achieve a robust clinical response. In this case, the models suggest that in comparison to monopolar stimulation, guarded bipolar stimulation would require a larger voltage to activate all of the fascicles. The models correctly predicted the clinical "sensation" and "functional" threshold voltages and the ratio between monopolar and bipolar configurations [33, 35] showing a significantly higher stimulus threshold for the guarded bipolar stimulation setting. The models indicated that this difference in threshold voltages stemmed from current being shunted between anodes and cathode through the interstitial fluid and encapsulation layers. These layers were located between the active electrodes and the nerve and are likely to vary in conductance and thickness as the reactive tissue response to the implanted device develops and stabilizes [36]. While the models were based on a fascicular structure with one primary and two secondary fascicles, other fascicular structures may occur in practice, especially when one considers the surgical location of the nerve-cuff assembly along the HGN. The models would indicate that for nerve segments with a higher number of fascicles that, as shown in Figure 5, monopolar (o-o and ---) configurations will be more successful at recruiting all of the fascicles than the case of bipolar (+-+) configurations.

The computational models of HGN stimulation were tuned to the clinical data in Figure 2 in terms of encapsulation tissue conductivity and encapsulation layer thicknesses [28, 29, 36, 37]. While the encapsulation tissue conductivity broadly changed the thresholds for axonal activation, we found that the encapsulation tissue thickness surrounding the cuff and especially at the nerve-cuff openings was a critical factor in aligning the relative ratios of axonal activation between guarded bipolar and grouped monopolar configurations. In clinical practice, the significance of the initial postimplant inflammatory response underlying formation of this encapsulation tissue is respected through the allotted time delays from nerve cuff placement to initial activation of stimulation and subsequent polysomnography-based titration of programming settings. However, previous studies have also noted changes in tongue motion patterns within the first year following implantation [33, 34], and these clinical observations may stem from changes in the interstitial fluid within the cuff and the encapsulation tissue both within the cuff and at the openings of the cuff. It is important to acknowledge that several other model parameters will likely vary from patient to patient, including the location of the cuff along the hypoglossal nerve; the number, size, and distribution of fascicles within the cuff; and the diameter, myelination, and excitability properties of the axons within each fascicle [38]. These parameters, in part, provide context for why one should expect the degree of variation in clinical stimulation thresholds as shown in Figure 2 among patients.

The interpatient variability of HGN computational model parameters emphasizes the importance of a standardized best-practice approach to therapy programming and troubleshooting to optimize clinical outcomes. Based on this data, a "one-size fits all" electrical programming will likely leave many patients suboptimally treated. During the initial device activation as well as subsequent follow-up visits, clinicians should synthesize available intraoperative information (e.g. individual neuroanatomy, cuff location along the nerve, cuff rotation) and clinical feedback (e.g. tongue motion, patient comfort, OSA outcome measures), and interpret both in the context of this model of electrical stimulation. Subsequent personalized and targeted therapy modifications have the potential to increase successful treatment in both the sleep clinic and sleep laboratory settings.

Postimplant healing and fibrosis over time, and associated changes in encapsulation layer thickness and conductivity, also support the need to closely monitor therapy long-term. From the initial device activation at 4-week postimplant, through the initial acclimation phase, through objective sleep testing in the first 6–12 months, and through the expected generator battery life of ten years or more, stimulation requirements may change. The model-based results of this study support a longitudinal care model, in which therapy outcomes and adherence are regularly reassessed, and stimulation parameters are adjusted accordingly. In summary, a firm understanding of the fundamentals of electrical stimulation parameters can help guide clinical decision-making and ultimately optimize long-term outcomes.

Acknowledgments

This work was sponsored in part by Inspire Medical Systems.

Disclosure Statement

Financial disclosure: Matthew Johnson, Yazan Dweiri, and Jason Cornelius have consulted for Inspire Medical Systems. Kingman Strohl is a site PI of the ADHERE postapproval registry sponsored by Inspire Medical Systems. Armin Steffen is a study investigator and received honoraria and travel expenses for invited talks on behalf of Inspire Medical Systems. Maria Suurna is an investigator on a postapproval clinical trial for Inspire Medical and received honoraria from Inspire Medical Systems. Ryan Soose is a study investigator and consultant for Inspire Medical Systems. Quan Ni, Michael Coleman, and John Rondoni are employees and stock shareholders of Inspire Medical Systems.

Non-financial disclosure: Kingman Strohl serves as a consultant or member of the advisory board for Sommetrics LLC, Seven Dreamers, Jazz Pharmaceuticals, Medscape, Up-to-Date. Armin Steffen serves as a consultant for Merz Pharmaceuticals and received honoraria for expert meetings from Proveca Ltd., Intersect Inc, and Onyx Ltd. Ryan Soose is a consultant for Smith & Nephew, Cryosa Inc., Invicta Medical, Galvani Bioelectronics, and Enhale Medical. All other authors have nothing to disclose.

References

1. Young T, *et al*. Epidemiology of obstructive sleep apnea. *Am. J. Respir. Crit. Care Med*. 2002;**165**;1217–1239.
2. Weaver TE, *et al*. Adherence to continuous positive airway pressure therapy: the challenge to effective treatment. *Proc Am Thorac Soc*. 2008;**5**(2):173–178.
3. Strollo PJ Jr, *et al*.; STAR Trial Group. Upper-airway stimulation for obstructive sleep apnea. *N Engl J Med*. 2014;**370**(2):139–149.
4. Steffen A, *et al*. Outcome after one year of upper airway stimulation for obstructive sleep apnea in a multicenter German post-market study. *Laryngoscope*. 2018;**128**(2):509–515.
5. Heiser C, *et al*.; ADHERE Registry Investigators. 2019 Post-approval upper airway stimulation predictors of treatment effectiveness in the ADHERE registry. *Eur Respir J*. **53**:1801405.
6. Boon M, *et al*.; ADHERE Registry Investigators. Upper airway stimulation for obstructive sleep apnea: results from the ADHERE Registry. *Otolaryngol Head Neck Surg*. 2018;**159**(2):379–385.
7. Schwab RJ, *et al*. Anatomic predictors of response and mechanism of action of upper airway stimulation therapy in patients with obstructive sleep apnea. *Sleep*. 2018;**41**(4):1–12. doi: 10.1093/sleep/zsy021.
8. Heiser C, *et al*. Functional outcome of tongue motions with selective hypoglossal nerve stimulation in patients with obstructive sleep apnea. *Sleep Breath*. 2016;**20**(2):553–560.
9. Grill WM, *et al*. Stimulus waveforms for selective neural stimulation. *IEEE EMBS Mag*. 1995; **14**(4):375–385.
10. McNeal DR. Analysis of a model for excitation of myelinated nerve. *IEEE Trans Biomed Eng*. 1976;**23**(4):329–337.
11. McIntyre CC, *et al*. Modeling the excitability of mammalian nerve fibers: influence of afterpotentials on the recovery cycle. *J Neurophysiol*. 2002;**87**(2):995–1006.
12. Rattay F. Analysis of models for extracellular fiber stimulation. *IEEE Trans Biomed Eng*. 1989;**36**(7):676–682.
13. Veltink PH, *et al*. A modeling study of nerve fascicle stimulation. *IEEE Trans Biomed Eng*. 1989;**36**(7):683–692.
14. Warman EN, *et al*. Modeling the effects of electric fields on nerve fibers: determination of excitation thresholds. *IEEE Trans Biomed Eng*. 1992;**39**(12):1244–1254.
15. Schiefer MA, *et al*. A model of selective activation of the femoral nerve with a flat interface nerve electrode for a lower extremity neuroprosthesis. *IEEE Trans Neural Syst Rehabil Eng*. 2008;**16**(2):195–204.
16. Kent AR, *et al*. Model-based analysis and design of nerve cuff electrodes for restoring bladder function by selective stimulation of the pudendal nerve. *J Neural Eng*. 2013;**10**(3):036010.
17. Helmers SL, *et al*. Application of a computational model of vagus nerve stimulation. *Acta Neurol Scand*. 2012;**126**(5):336–343.
18. Mourdoukoutas AP, *et al*. High-resolution multi-scale computational model for non-invasive cervical vagus nerve stimulation. *Neuromodulation*. 2018;**21**(3):261–268.
19. Tyler DJ, *et al*. Functionally selective peripheral nerve stimulation with a flat interface nerve electrode. *IEEE Trans Neural Syst Rehabil Eng*. 2002;**10**(4):294–303.
20. Gorman PH, *et al*. The effect of stimulus parameters on the recruitment characteristics of direct nerve stimulation. *IEEE Trans Biomed Eng*. 1983;**30**(7):407–414.
21. Fang ZP, *et al*. Alternate excitation of large and small axons with different stimulation waveforms: an application to muscle activation. *Med Biol Eng Comput*. 1991;**29**(5):543–547.
22. van den Honert C, *et al*. Generation of unidirectionally propagated action potentials in a peripheral nerve by brief stimuli. *Science*. 1979;**206**(4424):1311–1312.
23. Rattay F. Analysis of models for external stimulation of axons. *IEEE Trans Biomed Eng*. 1986;**33**(10):974–977.
24. Mackinnon SE, *et al*. Fascicular patterns of the hypoglossal nerve. *J Reconstr Microsurg*. 1995;**11**(3):195–198.
25. Vacher C, *et al*. Morphometric study of the cervical course of the hypoglossal nerve and its application to hypoglossal facial anastomosis. *Surg Radiol Anat*. 2004;**26**(2):86–90.
26. Grinberg Y, *et al*. Fascicular perineurium thickness, size, and position affect model predictions of neural excitation. *IEEE Trans Neural Syst Rehabil Eng*. 2008;**16**(6):572–581.
27. Heiser C, *et al*. Surgical anatomy of the hypoglossal nerve: a new classification system for selective upper airway stimulation. *Head Neck*. 2017;**39**(12):2371–2380.
28. Loeb GE, *et al*. Cuff electrodes for chronic stimulation and recording of peripheral nerve activity. *J Neurosci Methods*. 1996;**64**(1):95–103.
29. Grill WM, *et al*. Electrical properties of implant encapsulation tissue. *Ann Biomed Eng*. 1994;**22**(1):23–33.
30. Goding GS Jr, *et al*. Relief of upper airway obstruction with hypoglossal nerve stimulation in the canine. *Laryngoscope*. 1998;**108**(2):162–169.
31. Hursh JB. Conduction velocity and diameter of nerve fibers. *Am J Physiol*. 1939;**127**:131–139.
32. Safiruddin F, *et al*. Effect of upper-airway stimulation for obstructive sleep apnoea on airway dimensions. *Eur Respir J*. 2015;**45**(1):129–138.
33. Steffen A, *et al*. Tongue motion variability with changes of upper airway stimulation electrode configuration and effects on treatment outcomes. *Laryngoscope*. 2018;**128**(8):1970–1976.
34. Steffen A, *et al*. Upper airway stimulation for obstructive sleep apnea—can radiological position monitoring predict tongue motion one year after implantation? *HNO*. 2020;**68**(Suppl 1):11–16.
35. Kilic A. *Nervus Hypoglossus-stimulation in der Therapie der obstruktiven Schlafapnoe bei CPAP-Intoleranz:*

Zungenbewegungsmuster und Elektrodenkonfiguration. Erlangung der Doktorwürde Universität zu Lübeck; 2018; Katalog der Deutschen Nationalbibliothek of the German National Library (Deutsche National Bibliothek).
36. Grill WM, *et al*. Stability of the input-output properties of chronically implanted multiple contact nerve cuff stimulating electrodes. *IEEE Trans Rehabil Eng*. 1998;**6**(4):364–373.
37. Grill WM, *et al*. Neural and connective tissue response to long-term implantation of multiple contact nerve cuff electrodes. *J Biomed Mater Res*. 2000;**50**(2): 215–226.
38. Mogyoros I, *et al*. Strength-duration properties of human peripheral nerve. *Brain*. 1996;**119** (Pt 2): 439–447.